Published in "Proceedings of the National Academy of Sciences
108(51): 20790-20795, 2011" which should be cited to refer to this work.

Intragenic alternative splicing coordination is essential for *Caenorhabditis elegans slo-1* gene function

Dominique A. Glauser[a,b,1], Brandon E. Johnson[a,1], Richard W. Aldrich[c,2], and Miriam B. Goodman[a,2]

[a]Department of Molecular and Cellular Physiology, Stanford University School of Medicine, Stanford, CA 94305; [b]Department of Biology/Zoology, University of Fribourg, 1700 Fribourg, Switzerland; and [c]Section of Neurobiology, Center for Learning and Memory, University of Texas, Austin, TX 78712

Alternative splicing is critical for diversifying eukaryotic proteomes, but the rules governing and coordinating splicing events among multiple alternate splice sites within individual genes are not well understood. We developed a quantitative PCR-based strategy to quantify the expression of the 12 transcripts encoded by the *Caenorhabditis elegans slo-1* gene, containing three alternate splice sites. Using conditional probability-based models, we show that splicing events are coordinated across these sites. Further, we identify a point mutation in an intron adjacent to one alternate splice site that disrupts alternative splicing at all three sites. This mutation leads to aberrant synaptic transmission at the neuromuscular junction. In a genomic survey, we found that a UAAAUC element disrupted by this mutation is enriched in introns flanking alternate exons in genes with multiple alternate splice sites. These results establish that proper coordination of intragenic alternative splicing is essential for normal physiology of *slo-1* in vivo and identify putative specialized *cis*-regulatory elements that regulate the coordination of intragenic alternative splicing.

BK potassium channels | Slo1 channels

Alternative splicing is critical for diversifying protein function in eukaryotes (1). Recent advances in microarray technology and high-throughput sequencing suggest that alternate exon expression is often coregulated across many genes (2–4). Regulated splicing choices seem to depend on nucleotide sequences located in alternate exons or neighboring introns that recruit specialized splicing factors (5–7). Nearly every multiexon human gene contains alternate exons, and many genes contain multiple alternate splice sites (8, 9). For the latter category, the rules governing and coordinating alternative splicing across multiple intragenic splice sites are not well understood. Nonetheless, it seems likely that precise splicing decisions must be made at multiple loci to express the splice variant best tailored for each specific physiological context. Some evidence for such regulation has been obtained in cell-based systems and from a survey of ESTs in a few human genes with multiple alternate splice sites (10). However, lack of quantitative methods to address exon combinations at multiple sites in vivo has precluded a more detailed assessment of intragenic alternative splicing coordination.

Alternative splicing in the BK channel gene *slo-1* has tremendous implications for both physiology and pathophysiology, because it is known that individual isoforms are adapted to function in specific cell types, developmental stages, or are up-regulated in response to physiological stress (11–16). Here, we examined alternative splicing across all previously identified alternate splice sites of the *Caenorhabditis elegans slo-1* gene. Our goal was to determine whether alternative splicing events are independent or coregulated in the *slo-1* gene. The *slo-1* gene has 12 splice variants arising from alternative splicing at three sites (A, B, and C; Fig. 1*A*). At site A, a choice is made between two mutually exclusive exons: exon 9 (A1) or exon 10 (A2). At site B, exon 13 can be either skipped (B0) or included with two possible 5′acceptor sites (B1 or B2). At site C, exon 15 can be either skipped (C0) or included (C1). The combinatorial insertion of alternate exons across the A, B, and C sites is essential for the functional differences among *C. elegans slo-1* splice variants and for modulating interactions between functional protein domains (17). Because of these functional interactions, we hypothesized that alternative splicing is coordinated across multiple splice sites in *slo-1* to generate splice variants with specific physiological properties.

In this report, we derive a conditional probability model of alternative splicing to investigate the coordination of these events in the *slo-1* gene. Our model is based on empirical measurements of single alternate exons using conventional RT–quantitative PCR (qPCR) and of the expression of individual splice variants using an application of RT-qPCR called *Combinatorial Alternate Exon qPCR* (CAE-qPCR). By analyzing an intronic mutation that disrupts alternative splicing, we establish that proper coordination of alternative splicing across multiple sites is essential for BK channel function in vivo. Finally, we propose a mechanism involving a single *cis*-element present at all three splice sites in *slo-1* and in many other genes where multiple splicing decisions are likely to be similarly coordinated.

Results

Distribution of Splice Variants Expressed in Wild-Type *C. elegans*. All 12 possible *slo-1* alternate exon combinations have been detected by a cDNA cloning approach in *C. elegans* (17), but the relative expression of splice variants is unkown. To determine the distribution of alternate exon expression at each splice site in young adult animals, we used exon-specific dyed-based (SYBR green) RT-qPCR. The frequency with which each alternate exon appears in mature transcripts, considering one site at a time, is shown in Fig. 1*B*. Each alternate exon is present in at least 15% of total *slo-1* transcripts, suggesting that all alternate exons are expressed at nontrivial levels. However, this approach provides little insight into the relative expression levels of the 12 splice variant transcripts resulting from the combination of alternate exons at the three sites in *slo-1*. To investigate this question, we developed an application of probe hydrolysis (Taqman) RT-qPCR, CAE-qPCR, to quantify the expression of all *slo-1* variants. The method relies on specific hybridization of oligonuclotides at three sites along the target cDNA: two primer sets, targeting the 5′ alternate exon (A1 or A2) and the 3′ alternate exon (C0 or C1), respectively, and a set of probes, each targeting a specific alternate exon at site B (B0, B1, or B2) (Fig. 2*A*). Each of the 12 A-B-C primer and probe combinations detects only one variant, which we tested empirically using plasmids encoding each variant. We measured the impact of both nonspecific amplification (due to cross-hybridization among splice variants) and reagent titration effects (due to the parallel amplification of three variants per primer set) and controlled for both

Author contributions: D.A.G., B.E.J., R.W.A., and M.B.G. designed research; D.A.G. and B.E.J. performed research; D.A.G. and B.E.J. analyzed data; and D.A.G., B.E.J., and M.B.G. wrote the paper.

The authors declare no conflict of interest.

[1]D.A.G. and B.E.J. contributed equally to this work.

[2]To whom correspondence may be addressed. E-mail: raldrich@mail.utexas.edu or mbgoodman@stanford.edu.

This article contains supporting information online

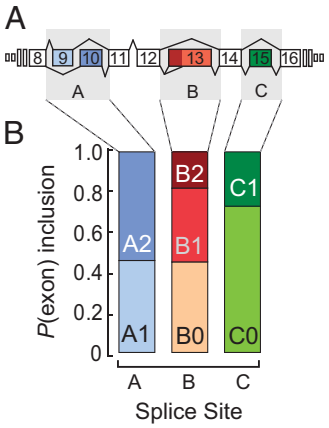

Fig. 1. Alternate exon distribution at individual splice sites in *slo-1*. (*A*) Schematic of the alternatively spliced region of *C. elegans slo-1* gene. Not to scale. (*B*) Proportional expression of each *slo-1* alternate exons as assessed by dye-based qPCR in adult worms (n = 5).

effects. Using this method, 10 of 12 variants were detected and reliably quantified from RNA obtained from whole adult worm lysates (*SI Materials and Methods*, Figs. S1–S3, Tables S1–S4).

Splicing Events at Individual Sites in the *slo-1* Gene Are Interdependent. A simple model for predicting the relative expression levels of each splice variant assumes that splicing events at sites A, B, and C occur independently from one another. In the independent-splicing model, the probability of expression of a given A;B;C splice variant is equal to the product of the splicing probabilities at each site:

$$P(\mathrm{A};\mathrm{B};\mathrm{C}) = P(\mathrm{A})*P(\mathrm{B})*P(\mathrm{C})$$

Using this model, we computed the expected expression of *slo-1* splice variants and compared the predicted values with those measured using CAE-qPCR (Fig. 2*B*). Values predicted by this model were outside the 99% confidence interval of the measured values for 9 of 10 detected variants. Thus, the simple independent-splicing model can be rejected, implying that splicing events are interdependent.

To characterize the relationship between splicing events, we systematically tested a series of conditional probability models in which the probability of exon choices at one site depends on the choices made at one or two other sites (Fig. S4 and Table S5). Single-interaction models were poor, but double-interaction models yielded better predictions. The better models more frequently included interaction effects of A on B, B on A, and A on C, and less frequently effects of C on A or C on B. Experimental data were therefore globally best fit by models assuming that exon choices at 5′ splice sites affect exon choices at 3′ sites. Consequently, we designed a final model in which the exon choice at site B depends on the exon inserted at site A, and the choice at site C depends on the exon combination at sites A and B. This best-fit interdependent-splicing model is formulated as follows:

$$P(\mathrm{A};\mathrm{B};\mathrm{C}) = P(\mathrm{A})*P(\mathrm{B}|\mathrm{A})*P(\mathrm{C}|\mathrm{AB})$$

This model most closely matches the experimental distribution of *slo-1* splice variants in wild-type adults (Fig. 2*C* and Fig. S4). To learn more about the interdependence of alternative splicing, we examined the impact of an intronic *slo-1* mutation that changes alternative splicing.

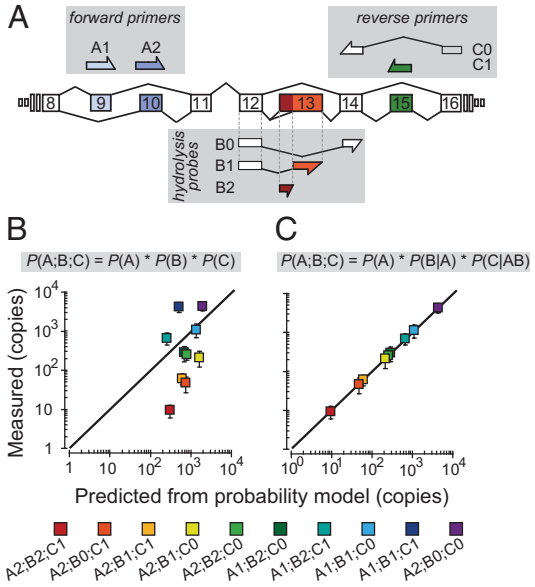

Fig. 2. Alternative splicing across three sites is coordinated in *slo-1*. (*A*) Schematic of the recognition sequences used in the CAE-qPCR approach. Combinatorial use of these primers and probes allows the detection of all 12 *slo-1* splice variants. (*B* and *C*) Copy numbers of each *slo-1* splice variant were measured by CAE-qPCR in adult worms and their means plotted against the corresponding predicted values. Predictions were calculated according to the depicted formulas. Error bars are 99% confidence intervals of the means (n = 5). The solid line shows the relationship expected for a perfect match between the two datasets. Probability values for the conditional probability model were: P(A1) = 0.459, P(A2) = 0.541, P(B0|A1) = 0.000, P(B1|A1) = 0.846, P(B2|A1) = 0.154, P(B0|A2) = 0.891, P(B1|A2) = 0.055, P(B2|A2) = 0.054. P(C0|A1B0) = 0.000, P(C1|A1B0) = 0.000, P(C0|A1B1) = 0.208, P(C1|A1B1) = 0.792, P(C0|A1B2) = 0.300, P(C1|A1B2) = 0.700, P(C0|A2B0) = 0.989, P(C1|A2B0) = 0.011, P(C0|A2B1) = 0.776, P(C1|A2B1) = 0.224, P(C0|A2B2) = 0.964, and P(C1|A2B2) = 0.036.

Intronic Mutation in *slo-1* Alters Synaptic Transmission. We designed a forward genetic screen to identify partial loss-of-function *slo-1* mutations that rely on aldicarb-induced paralysis and a sensitized genetic background. Aldicarb inhibits acetylcholinesterase, increases muscle activation, and causes rigid paralysis over a period of several hours. Previously characterized loss-of-function alleles of *slo-1* cause animals to be hypersensitive to the paralytic effect of aldicarb and increase acetylcholine release at the neuromuscular junction (18, 19). The majority of existing *C. elegans slo-1* alleles are thought to be null. This observation suggests that although partial loss-of-function mutations may be difficult to detect in behavioral screens in a wild-type background, such mutations could be revealed in animals with a reduced calcium influx into motor neurons. We identified *unc-2 (ra612)* as a mutation likely to produce the needed decrease in presynaptic Ca^{2+} influx. The *unc-2* gene is expressed in motor neurons and encodes the α subunit of a voltage-gated Ca^{2+} channel gene. The *ra612* allele causes animals to be resistant to aldicarb, decreases channel voltage sensitivity, and accelerates inactivation (20). Thus, *unc-2(ra612)* opposes the paralyzing consequences of acetylcholinesterase inhibition, allowing the paralytic phenotype of partial loss-of-function *slo-1* mutants to be revealed.

We recovered a total of 11 alleles that failed to complement *slo-1(null)* in our screen, including *pg52*. Sequencing the *slo*-1 gene in *pg52* revealed a wild-type coding sequence and a single nucleotide mutation in the 67bp intron between exon 12 and alternate exon 13 at site B (Fig. 3*A*). The *slo-1(pg52)* single mutant is hypersensitive to aldicarb compared with wild-type animals, but the phenotype is less severe than *slo-1(null)* (Fig. 3*B*), indicating that the *pg52* mutation confers a partial reduction of BK channel function.

Mutation Near Site B Disrupts Exon Expression at All Sites. Because the *slo-1* gene in *pg52* animals has a wild-type mRNA coding sequence, the mutation could alter BK channel function through

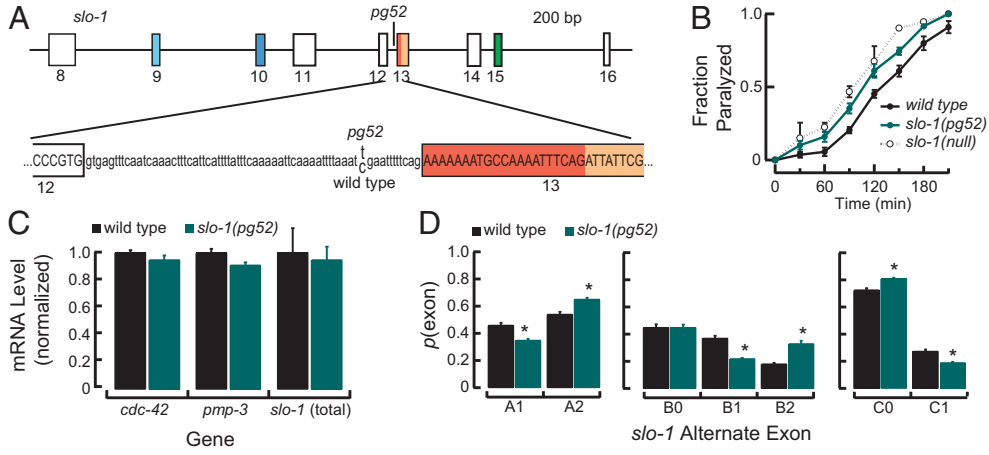

Fig. 3. *pg52* intronic mutation disrupts the function of the neuromuscular junction and *slo-1* alternate exon expression. (*A*) Schematic (to scale) of the *slo-1* gene locating the *pg52* mutation (C to T transition) and surrounding sequence. (*B*) Aldicarb-induced paralysis in wild-type animals and *slo-1(pg52)*. Worms were incubated for the indicated period on plates containing 0.5 mM aldicarb. Points are the average ± SEM of at least three assays. *slo-1(null)* is *slo-1(js379)*. (*C*) Total *slo-1* and reference gene transcript levels were measured by RT-qPCR targeting constitutive exons in adult worms. For total *slo-1*, the region between exons 16 and 18 was targeted. For each gene, results were normalized to the wild-type level and expressed in relative units. Bars are mean ± SEM ($n = 5$). No significant difference was detected between wild-type and *pg52* adults (Student *t* test). (*D*) Alternate exons were quantified in wild-type (N2) and *slo-1(pg52)* animals by dye-based qPCR. Two-way ANOVAs revealed significant Exon-type × Genotype interaction effects at all three sites [site A: $F_{(1,16)} = 56.30$, $P < 0.01$; site B: $F_{(1,16)} = 36.75$, $P < 0.01$; site C: $F_{(1,16)} = 75.03$, $P < 0.01$]. Bars are mean ± SEM ($n = 5$). *$P < 0.001$ vs. wild type by Bonferroni post hoc tests.

changes in total transcript levels, variations in splicing, or both. We measured total *slo-1* transcript levels by RT-qPCR targeting a constitutive region between exon 16 and 18, present in all variants. In parallel, we assessed two control genes, *cdc-42* and *pmp-3*, whose expression is known to be very stable (21). We found that all three transcripts were expressed at indistinguishable levels in *pg52* mutants and wild-type animals (Fig. 3*C*). Thus, the *slo-1(pg52)* phenotype is unlikely to be explained by a general decrease in *slo-1* expression.

Next, we determined whether the *pg52* mutation affects alternative splicing. Absolute quantification of each of the seven alternate exons by RT-qPCR shows that *pg52* decreases the abundance of B1-type transcripts and increases the abundance of B2-type transcripts, but has no detectable effect on the level of B0-type transcripts (Fig. 3*D*). Interestingly, the effect of the *pg52* mutation was not limited to splice site B. *slo-1(pg52)* animals also contained proportionally fewer A1-type and C1-type transcripts compared with wild-type animals, providing further support that alternative splicing is coordinated across multiple sites.

To better characterize how *pg52* affects exon expression, we measured the *slo-1* splice variant expression by CAE-qPCR from mutant animals and compared these values with wild type. As observed for the expression of individual alternate exons (Fig. 3*D*), *pg52* affects alternative splicing at all three sites, significantly altering the expression pattern of splice variants in adult animals (Fig. 4 *A*–*C*). The most prominent effect of the mutation is a systematic 67% ± 11% reduction in the four B1-type splice variants, which is consistent with a local effect of the mutation near the B1/B2 splicing acceptor site (see fold changes in Fig. 4*A*). A1;B1;C1 expression was significantly lower in *slo-1(pg52)* and represents the largest absolute change in copy number caused by the mutation (Fig. 4*B*). The down-regulation of A1;B1;C1 accounts for the majority of the proportional decline in A1-type and C1-type splice variants reported in Fig. 3*D*.

If *pg52* only shifted the probability of exon use at splice site B such that B2 was preferentially expressed over B1, then the down-regulation of each B1-type exon would be matched by a complementary up-regulation of the corresponding B2-type splice variants. This prediction is not supported by our data: two of the four B2 containing variants are down-regulated (Fig. 4*A*). These findings indicate that *pg52* has a more complex effect on splicing than a simple change in exon choice at site B.

Intragenic Coordination of Alternative Splicing Is Altered by the *pg52* Mutation in *slo-1*. To better understand the effect of *pg52* on alternative splicing, we analyzed the conditional probabilities that exon selection at one site coincides with a specified pair of alternate exons at the two other sites. We compared the nonconditional probabilities (Fig. 4*D*) and the conditional probabilities for each possible choice and context (Fig. 4*E*) for wild type (N2) and *pg52*. For both genotypes, the conditional probability profiles differ dramatically from the nonconditional probabilities. This difference directly reflects the fact that exon selection events at all sites influence each other (compare Fig. 4 *D1* with *E1*, *D2* with *E2*, and *D3* with *E3*).

At first glance, the conditional probability patterns appear very similar between the two genotypes. For instance, A2 is always present in B0;C0-type and B0;C1-type splice variants in both wild type and *slo-1(pg52)*, whereas A1 is present in a majority of B1- and B2-type splice variants (Fig. 4*E1*). Therefore, some features underlying the interdependent regulation of splicing across sites are intact in *pg52*. However, the conditional probabilities of exon use are not identical across all combinations. The most striking difference in exon selection probabilities between wild type and *pg52* is among the A1;B2-type splice variants. In wild type, C0 is strongly disfavored in the A1;B2 context, and the corresponding conditional probability (Fig. 4*E3*) strongly diverges from the nonconditional probability (Fig. 4*D3*). In *pg52*, however, C0 is no longer disfavored, and the corresponding conditional probability is similar to the nonconditional probability, indicating a disruption of the splicing coordination.

Following the same analysis as for wild type, we calculated the predicted variant expression values from conditional probability-based models for the *pg52* mutant and compared them with measured values (Table S6). As found for wild type, the independent splicing model cannot account for the *pg52* splice variant expression pattern (Fig. S5). Consistent with a partial disruption of splicing coordination, the match between the values obtained with the best-fit model (Fig. 2*C*) for *pg52* data is weaker than for wild type (100% for wild type, Fig. 2*C*, vs. only 70% for *pg52*, Fig. S5).

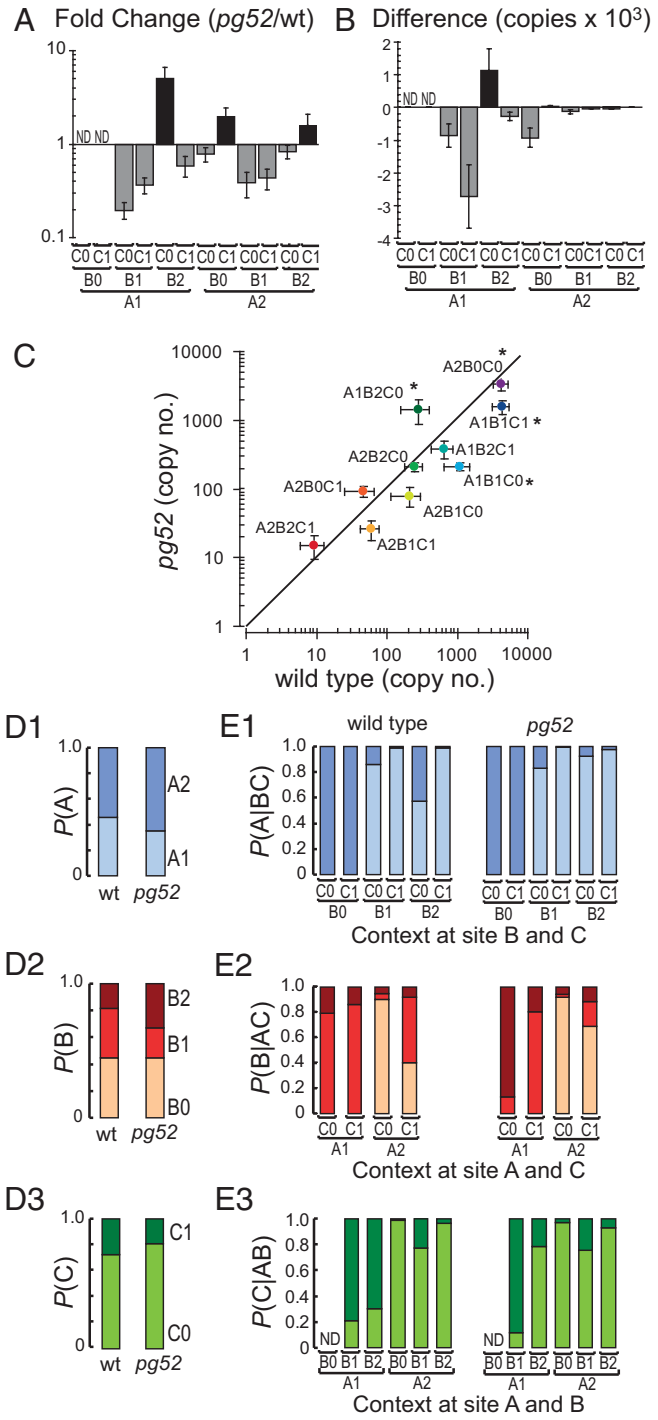

Fig. 4. *pg52* mutation affects the B1/B2 ratio and splicing coordination across A, B, and C sites. (*A* and *B*) Fold change in expression and absolute difference in copy numbers, respectively, were calculated from CAE-qPCR data for each variant. (*C*) Copy numbers of each detectable variant in *pg52* mutants were plotted against their respective number in N2 animals. Error bars are 99% confidence intervals (n = 5). A two-way ANOVA indicated a significant Variant × Genotype interaction effect [$F_{(9,80)}$ = 16.24, P < 0.01]. *P < 0.01 between the two genotypes by Bonferroni post hoc tests. Data are averages ± SD. (*D1–3*) Nonconditional probabilities are the same as in Fig. 3*D* and are presented here for comparison (*E1–3*) Conditional probabilities of splicing decisions at a given site are plotted as a function of the context at the other two sites.

Collectively, our data show that the change in *slo-1* splice variant expression in the *pg52* mutant results from two mechanisms: first, a systematic decrease in the inclusion of B1 exons; second, a partial disruption of splicing coordination over the three sites.

***pg52* Disrupts a Putative *cis*-Regulatory Element Enriched in Introns Flanking Alternate Exons in Genes with Multiple Alternate Splice Sites.** To better understand the coupling mechanism linking splicing at sites A, B, and C, we analyzed the sequence disrupted by the *pg52* mutation. Previous research identified many pentameric and hexameric motifs located in introns, believed to regulate alternative splicing (22). We used a similar approach and examined the distribution within *slo-1* of all of the possible pentameric and hexameric elements encompassing the base pair substitution in *pg52*. Strikingly, out of six occurrences of the UAAAUC element, three were located near site A, one near site B (converted to UAAAUU in *pg52*), and one near site C (Fig. 5*A*).

To evaluate whether the UAAAUC motif might function as a *cis*-regulatory element coordinating alternative splicing across multiple sites in other genes, we analyzed the distribution of this motif in introns flanking alternate exons in the *C. elegans* genome. The comparison was made between genes with single alternate splice sites (SASS genes) and genes with multiple alternate splice sites (MASS genes). We found that UAAAUC-containing introns were slightly yet significantly enriched in the 651 MASS genes compared with the 1,191 SASS genes we analyzed in the *C. elegans* genome (1.5 enrichment, $P < 10^{-6}$, by Fisher's exact test). Because the enrichment is modest, we hypothesized that UAAAUC-dependent splicing regulation might target a specific subset of genes, such as those containing multiple instances of the UAAAUC motif, as found in *slo-1*. We found 48 MASS genes that fit the criterion of having UAAAUC motifs in at least two alternate introns. Functional annotation analysis for these genes revealed a strong enrichment of genes involved in locomotion (17 genes), embryonic and larval development (19 genes), growth and reproduction (22 genes), and morphogenesis (9 genes; Fig. 5*B* and Table S7). These results indicate that the UAAAUC element is not ubiquitous among the MASS genes but suggest that it could function to coordinate alterative splicing in a few defined groups of functionally related genes.

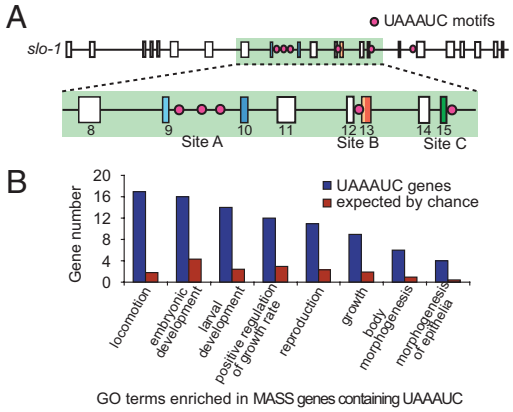

Fig. 5. Bioinformatic analysis of the UAAAUC element. (*A*) Schematic of the location of UAAAUC elements along the *slo-1* gene. Five of six elements are located in introns flanking A, B, and C alternative splice sites (highlighted in green and magnified). (*B*) GO terms were analyzed for a group of MASS genes with more than one alternate splice site flanked by a UAAAUC-containing intron (blue). Number of hits expected by chance (red) were calculated on the whole genome *C. elegans* annotation repository (Wormbase release WS-220). Categories with a significant enrichment in the UAAAUC group are depicted (P < 0.01, by Fisher's exact test with correction for multiple comparisons).

Discussion

Proper Splicing Coordination in *slo-1* Is Critical for BK Channel Function. At least 25% of human genes have more than one alternate splice site (10), suggesting that coordination of splicing events has the potential to regulate combinatorial proteomic diversity. The *slo1* BK channel gene is a particularly interesting case: multiple alternative splice sites that target the same protein region are found across all examined species from nematodes to human (23). In a parallel study (17), we evaluated the biophysical properties of 12 *C. elegans* SLO-1 splice variants and determined that the protein subdomains targeted by alternative splicing functionally interact to modulate BK channel kinetics, Ca^{2+} sensitivity, and gating free energy. In particular, we found that A2-type channels activate more slowly and at higher voltages than the corresponding A1-type channels, if and only if alternate exons are inserted at site B or C. In the present study, we demonstrate that the splicing events at all three sites strongly depend on each other and that mechanisms leading to preferential expression of given alternate exon combinations are engaged. We also show that a single nucleotide mutation in the putative UAAAUC regulatory element alters these interdependent splicing events, increasing the proportion of A2-type splice variants. As revealed by analysis of the voltage- and calcium-dependence of heterologously expressed BK channel variants (17), A2-type variants activate more slowly and are less sensitive to intracellular calcium. Thus, we predict that the *pg52* mutation decreases presynaptic BK channel activity by increasing the proportion of A2-type splice variants. This prediction is consistent with the impaired synaptic transmission at the neuromuscular junction observed in *pg52* mutants. We conclude that coordinated alternative splicing is critical for SLO-1 BK channel function at the neuromuscular junction in vivo.

Impact of *pg52* Mutation at Site B. One of the effects of *pg52* is an increase in the B2/B1 alternate exon ratio. In wild type, B2-type variants are the least abundant and were only recently identified in a parallel study by cloning methods (17). Thus, the B1 acceptor sequence is preferentially used over the B2 site in wild-type animals. The *pg52* mutation changes the genomic sequence very close to the B2 acceptor sequence and may favor the B2 exon definition by inducing a structural change, by inhibiting the binding of a putative UAAAUC-binding factor, or both. Although we favor these mechanisms, we cannot exclude the possibility that *pg52* uncovers an additional cryptic splice site in *slo-1*.

Coupling Mechanisms Between Multiple Splicing Sites. Polar effects across two splice sites have been reported before, whereby exon skipping at a site proximal to a gene promoter affects exon skipping at a more distal site (10). The proposed mechanism involves the cooperative recruitment of splicing factors on the nascent transcript at both sites and the influence of their order of appearance during transcription. In the case of *slo-1*, we observed bidirectional effects with respect to transcription polarity, because the *pg52* mutation near site B affected splicing both upstream (5′) at site A and downstream (3′) at site C. However, because all three sites are relatively close, predicting their actual order of availability to the splicing machinery is not straightforward. Potential mechanisms underlying the interdependent exon definition include the competitive binding of splicing factors present at nonsaturating concentrations, or the cooperative recruitment of splicing factors with potential direct interactions between the RNA–protein complexes from distinct splice sites. Future studies aiming at identifying the putative UAAAUC-binding, transacting factor will be very helpful in understanding the splicing coordination mechanism in *slo-1*.

UAAAUC Element. The UAAAUC element is enriched in introns flanking alternate exons in genes with multiple alternative splice sites in *C. elegans*. We observed that this enrichment in MASS genes was more pronounced for specific, functionally related sets of genes (Fig. 5*B*). This observation leads us to speculate that UAAAUC-dependent splicing coordination might be used preferentially in distinct tissues (as in neurons controlling locomotion) or at distinct developmental stages (as in embryogenesis and larval development). Similar to the present example, we propose that other splicing regulatory motifs are specialized for coordinating alternative splicing across MASS genes more generally. We also anticipate the existence of MASS genes in which independent splicing prevails and provides a better match to physiological requirements. Global, comprehensive analyses of splicing coordination and putative regulatory motifs will be required to determine whether splicing coordination is the rule or the exception and whether specialized regulatory motifs are com mon or rare.

In conclusion, our study provides evidence for intragenic splicing coordination in the *slo-1* gene, identifies a regulatory sequence in a short intron that is required for coordinated splicing, and demonstrates that this mechanism is critical for the gene product function. The quantitative approach undertaken here can be generally applied to determine how alternative splicing is regulated across multiple loci within single MASS genes and to ultimately better understand how these mechanisms are engaged to regulate splicing across tissues, during development, and through environmental changes.

Materials and Methods

***C. elegans* Strains, Mutagenesis, and Behavioral Assays.** The following *C. elegans* strains were used and maintained according to standard procedures (24): wild-type (N2, Bristol), NM1968 *slo-1(js379)* V, DM612 *unc-2(ra612)* X, GN4 *slo-1(js379)* V; *unc-2(ra612)* X, *slo-1(pg52)* V; *unc-2(ra612)* X, and GN52 *slo-1(pg52)* V. We screened *unc-2(ra612)* mutants (gift of T. Snutch, Vancouver, Canada) for extragenic mutations that increased sensitivity to the paralytic agent aldicarb, as described in *SI Materials and Methods*. A total of 32 mutants were recovered in this screen. On the basis of their failure to complement *slo-1 (js379)* null mutants, 11 of these mutants are alleles of *slo-1*, including the *pg52* allele characterized in detail here. Wild-type and mutant animals were tested for their sensitivity to aldicarb using the parallel worm tracker (25). The full assay method is provided in *SI Materials and Methods*.

cDNA Sample Preparation and qPCR Procedures. Full experimental procedures are presented in *SI Materials and Methods*. Briefly, total RNA was extracted from populations of young adult animals grown on standard nematode growth medium (NGM) growth plates seeded with OP-50 *Escherichia coli* bacteria. Five independent biological replicates (worm homogenates) were analyzed for each genotype. All qPCR experiments used a StepOnePlus apparatus (Applied Biosystems) housed in the Protein and Nucleic Acid (PAN) Facility at Stanford University. To measure and control for the total amount of cDNA in individual samples, we quantified expression of two reference genes, *cdc-42* and *pmp-3*, as previously described (21). Standard curves for absolute quantification (made by serial dilution of plasmids carrying each of the 12 *slo-1* splice variants) as well as *No reverse transcriptase* and *No cDNA template* controls were included in each PCR run. Primers were synthesized at the PAN Facility (Stanford University), and probes were synthesized at Biosearch Technologies. Their design, sequences, and validation are presented in *SI Materials and Methods*.

Probability Modeling. Nonconditional probabilities were calculated from the frequency of each splice variant in the total pool of *slo-1* transcripts. Conditional probabilities were calculated from the frequency of each variant in subgroups. For example, the probability of B1 knowing the occurrence of A1 was calculated as follows:

$$P(\text{B1}|\text{A1}) = P(\text{all A1;B1 containing variants})/P(\text{all A1 containing variants})$$

The predicted probability of a given variant was calculated by multiplying the probability (conditional or nonconditional) of exon choices at the three sites.

Bioinformatic Analysis. We retrieved the coordinates and sequences of all introns from genes with multiple isoforms reported in Wormbase (release WS-220; 3,115 genes). Intron positions were computed to remove constitutive

introns and alternate sequences resulting from alternative transcriptional start or termination. Among the list of alternate introns, we sorted intronic sequences located in genes where alternative splicing occurs at more than one site (651 MASS genes) or at only one site (1,191 SASS genes). The number of genes carrying at least one UAAAUC motif in introns flanking alternate exons was determined for both groups. Enrichment statistical significance in the MASS gene group relative to the SASS gene group was evaluated by Fisher's exact test. We used WormMart (searching Wormbase release WS-220) to retrieve Gene Ontology (GO) terms for 48 MASS genes in which the UAAAUC motif was detected in two or more alternate introns. The relative enrichment of GO terms was assessed using Fischer's exact test with Bonferroni's correction for multiple tests.

ACKNOWLEDGMENTS. We thank Andrew Davies for *slo-1* sequencing primer sequences; Zhao-Wen Wang for the SLO-1(A2;B0;C1) plasmid; Elise S. Dan-Glauser for statistical consultations; wormbase.org; and Colin Thacker, Terry Snutch, Michael Nonet, and the Caenorhabditis Genetics Center, which is funded by the National Institutes of Health (NIH) National Center for Research Resources, for strains. This work was supported by fellowships from the A. P. Sloan Foundation, Donald D. and Delia E. Baxter Foundation, NIH Grants NS047715 and NS061147, and Grant MDA#4206 from the Muscular Dystrophy Association (to M.B.G.); a predoctoral Ruth L. Kirschstein Fellowship from the National Institute of Neurological Disorders and Stroke (to B.E.J.); and Fellowships for Prospective Researchers from the Swiss National Science Foundation (to D.A.G.).

1. Stamm S, et al. (2005) Function of alternative splicing. *Gene* 344:1–20.
2. Blencowe BJ (2006) Alternative splicing: New insights from global analyses. *Cell* 126: 37–47.
3. Sultan M, et al. (2008) A global view of gene activity and alternative splicing by deep sequencing of the human transcriptome. *Science* 321:956–960.
4. Barberan-Soler S, Medina P, Estella J, Williams J, Zahler AM (2011) Co-regulation of alternative splicing by diverse splicing factors in *Caenorhabditis elegans*. *Nucleic Acids Res* 39:666–674.
5. Stamm S (2008) Regulation of alternative splicing by reversible protein phosphorylation. *J Biol Chem* 283:1223–1227.
6. Chen M, Manley JL (2009) Mechanisms of alternative splicing regulation: Insights from molecular and genomics approaches. *Nat Rev Mol Cell Biol* 10:741–754.
7. House AE, Lynch KW (2008) Regulation of alternative splicing: more than just the ABCs. *J Biol Chem* 283:1217–1221.
8. Pan Q, Shai O, Lee LJ, Frey BJ, Blencowe BJ (2008) Deep surveying of alternative splicing complexity in the human transcriptome by high-throughput sequencing. *Nat Genet* 40:1413–1415.
9. Wang BB, O'Toole M, Brendel V, Young ND (2008) Cross-species EST alignments reveal novel and conserved alternative splicing events in legumes. *BMC Plant Biol* 8:17.
10. Fededa JP, et al. (2005) A polar mechanism coordinates different regions of alternative splicing within a single gene. *Mol Cell* 19:393–404.
11. Chen L, et al. (2005) Functionally diverse complement of large conductance calcium- and voltage-activated potassium channel (BK) alpha-subunits generated from a single site of splicing. *J Biol Chem* 280:33599–33609.
12. Saito M, Nelson C, Salkoff L, Lingle CJ (1997) A cysteine-rich domain defined by a novel exon in a slo variant in rat adrenal chromaffin cells and PC12 cells. *J Biol Chem* 272:11710–11717.
13. Shipston MJ, Duncan RR, Clark AG, Antoni FA, Tian L (1999) Molecular components of large conductance calcium-activated potassium (BK) channels in mouse pituitary corticotropes. *Mol Endocrinol* 13:1728–1737.
14. MacDonald SH, Ruth P, Knaus HG, Shipston MJ (2006) Increased large conductance calcium-activated potassium (BK) channel expression accompanied by STREX variant downregulation in the developing mouse CNS. *BMC Dev Biol* 6:37.
15. Zhu N, et al. (2005) Alternative splicing of Slo channel gene programmed by estrogen, progesterone and pregnancy. *FEBS Lett* 579:4856–4860.
16. McCartney CE, et al. (2005) A cysteine-rich motif confers hypoxia sensitivity to mammalian large conductance voltage- and Ca-activated K (BK) channel alpha-subunits. *Proc Natl Acad Sci USA* 102:17870–17876.
17. Johnson BE, et al. (2011) Alternatively spliced domains interact to regulate BK potassium channel gating. *Proc Natl Acad Sci USA* 108:20784–20789.
18. Mahoney TR, Luo S, Nonet ML (2006) Analysis of synaptic transmission in *Caenorhabditis elegans* using an aldicarb-sensitivity assay. *Nat Protoc* 1:1772–1777.
19. Wang ZW, Saifee O, Nonet ML, Salkoff L (2001) SLO-1 potassium channels control quantal content of neurotransmitter release at the *C. elegans* neuromuscular junction. *Neuron* 32:867–881.
20. Mathews EA, et al. (2003) Critical residues of the *Caenorhabditis elegans unc-2* voltage-gated calcium channel that affect behavioral and physiological properties. *J Neurosci* 23:6537–6545.
21. Hoogewijs D, Houthoofd K, Matthijssens F, Vandesompele J, Vanfleteren JR (2008) Selection and validation of a set of reliable reference genes for quantitative sod gene expression analysis in *C. elegans*. *BMC Mol Biol* 9:9.
22. Kabat JL, et al. (2006) Intronic alternative splicing regulators identified by comparative genomics in nematodes. *PLoS Comput Biol* 2:e86.
23. Fodor AA, Aldrich RW (2009) Convergent evolution of alternative splices at domain boundaries of the BK channel. *Annu Rev Physiol* 71:19–36.
24. Stiernagle T (2006) Maintenance of *C. elegans*. *WormBook* Feb 11:1–11.
25. Ramot D, Johnson BE, Berry TL, Jr., Carnell L, Goodman MB (2008) The Parallel Worm Tracker: A platform for measuring average speed and drug-induced paralysis in nematodes. *PLoS ONE* 3:e2208.